# Critical zone storage control on the water ages in ecohydrological outputs

**S. Kuppel [1,2,3], D. Tetzlaff [4,5,3], M. P. Maneta [6], and C. Soulsby [3,4]**

[1] Institut de Physique du Globe de Paris, CNRS UMR 7154 - University of Paris, 75231 Paris, France.

[2] INRAE, RiverLy, 69625 Villeurbanne, France.

[3] Northern Rivers Institute, University of Aberdeen, Aberdeen, AB24 3UF, United Kingdom.

[4] Leibniz Institute of Freshwater Ecology and Inland Fisheries, Berlin, 12587, Germany.

[5] Department of Geography, Humboldt University Berlin, Berlin, 10099, Germany.

[6] Geosciences Department, University of Montana, Missoula, MT 59812-1296, USA.

Corresponding author: Sylvain Kuppel (sylvain.kuppel@inrae.fr)

## Key Points

- Age since precipitation displays inverse storage effect in stream, but not transpiration and soil evaporation, in a humid northern catchment
- Hysteresis between storage and the age of transpired water suggests cross-season carryover, despite weak hydroclimatic seasonality
- Downslope water subsidies result in valley bottom having weaker storage-age relationships than seen in freely-draining hillslopes

## Plain Language Summary

Knowing how much time water spends in a landscape (its "age") helps understanding how water travels through it. These dynamics inform of the stability of water resources for ecosystems and societies, and of their vulnerabilities under climate and land use changes. Water ages may vary depending on how wet or dry a location gets between seasons and years. We thus need to learn more about the demographics ("how much and how old?") of the water used by plants, evaporated from soils, and flowing in streams, but it is often impossible to monitor the heterogeneity of water pathways within landscapes. Addressing this challenge, we used a numerical model built upon coupling ecohydrological processes and that maps landscape locations. We adjusted this model using multiple datasets in a catchment representative of humid boreal environments where climate and vegetation are rapidly changing. We found markedly different aging patterns between water escaping the system through the plants, soils, and stream, depending on water storage status. This changing duration of water movement also differs between the catchment as a whole and its parts. This method can be used to better understand the multiple ways in which water moves through landscapes, in current and future conditions.


## Abstract

Spatially-explicit knowledge of the origins of water resources for ecosystems and rivers is challenging when using tracer data alone. We use simulations from a spatially-distributed model calibrated by extensive ecohydrological datasets in a small, energy-limited catchment, where hillslope-riparian dynamics are broadly representative of humid boreal headwater catchments that are experiencing rapid environmental transition. We hypothesize that in addition to wetness status, landscape heterogeneity modulates the water pathways that sustain ecosystem function and streamflows. Simulations show that catchment storage inversely controls streamwater ages year-round, but only during the drier seasons for transpiration and soil evaporation. The ages of these evaporative outputs depend much less on wetness status in the oft-saturated riparian soils than on the freely-draining hillslopes that subsidize them. This work highlights the need to consider local dynamics and time-changing lateral heterogeneities when interpreting the ages, and thus the vulnerability, of water resources feeding streams and ecosystems in landscapes.


## 1 Introduction

The age of water as it is routed along different pathways within a landscape, i.e., the transit time to exit from entry as zero-aged inputs (e.g., precipitation in catchment hydrology, or groundwater recharge in hydrogeology), has long been recognized as an important metric that explicitly indexes linkages between stores and fluxes (Bolin & Rodhe, 1973; Hrachowitz et al., 2016). In particular, the demographics of the water ultimately used by vegetation or evaporated from the soil directly informs on the "temporal depth" of the resources supporting life and the biogeochemical cycles in the shallow underground of the critical zone (Sprenger et al., 2019). From seasonal carryover of precipitation inputs (Allen et al., 2019; Kuppel et al., 2017) to vegetation responses to interannual variations in water availability (Bales et al., 2018; Chitra-Tarak et al., 2018; Hahm et al., 2019), knowing the ages of this "green water" (i.e., not feeding streamflow nor deep recharge; (Falkenmark & Rockström, 2006) would crucially help in assessing the vulnerability of natural vegetation communities to drought and climatic stress, and the sustainability of managed systems (e.g. timber and rain-fed agrosystems).

Quantifying the demographics of green water has however received little attention (Soulsby, Birkel, et al., 2016), due to the difficulty of directly disentangling the components of green water dynamics outside of carefully controlled experiments (Evaristo et al., 2019). Most of the analytical developments regarding transit time characterization have remained focused on dating streamwater or groundwater using concentrations in environmental tracers (Bethke & Johnson, 2008; McGuire & McDonnell, 2015), for which advanced analytical frameworks resolve the water age distribution of outputs or of water stores, sometimes linking the two (Benettin et al., 2013; Botter, 2012; Harman, 2015, 2019; Hrachowitz et al., 2013; Jasechko, 2019; Jasechko et al., 2016; Rinaldo et al., 2015). These efforts have highlighted the dynamic link between storage dynamics and water ages in streamflow as a key signature of hydrological functioning, yet there is currently no framework to assess how such relationships would translate for spatially-distributed outputs such as plant transpiration and soil evaporation. In most cases water ages are interpreted as a mixture of water being partitioned between shallower and deeper flow paths (e.g., surface runoff, interflow, groundwater lateral flow) in a lumped description of the spatial domain. This vertical view, however, remains to be articulated with the lateral heterogeneity in critical zone attributes (e.g. land cover type, topographic position, subsurface properties, vegetation phenology, slope exposure) and resulting variability of pathways, mixing and storages. This will help not only avoiding misinterpretation of apparent water ages dynamics at spatially aggregated scales (Kirchner, 2016; Soulsby et al., 2015), but, crucially, better capturing heterogeneous ecohydrological responses to environmental changes observed within real-world landscapes (Bales et al., 2018).

Addressing the crucial issue of water resources vulnerabilities in the critical zone requires bridging the wealth of information from ecohydrological measurements of water composition, fluxes and stores with the capacities of process-based models to inform on internal hydrological states (Maneta et al., 2018; Wilusz et al., 2020; Yang et al., 2018). We do so using a novel spatially-distributed model where the time-varying water ages in ecohydrological fluxes are dynamically derived from mixing equations at the grid cell level. It is applied in a small (3.2 km$^2$) energy-limited, humid headwater catchment where the model has been calibrated and validated using exceptionally diverse and long-term datasets (Kuppel et al., 2018b, 2018a). Our analysis shows not only that the seasonal changes in landscape wetness exert a distinctive control on the ages of water transpired by plants, evaporated from the soil and flowing in the stream, but also that landscape position and lateral heterogeneity between hydropedological units play a role in modulating the availability of younger replenishable water and older water that renews more slowly. An implication is that landscape heterogeneity is a strong control on the relative importance of flow pathways that contribute water for ecosystem health and streamflow generation. The effect of landscape heterogeneity may thus obscure the actual impact of climate variability on the water sources that sustain ecosystem function. Our findings may help assess the true vulnerability of ecosystem water supplies to precipitation variability and land cover change, thus advancing our understanding of hydrologic resilience in regions experiencing environmental transition.

## 2 Materials and Methods

### 2.1 Study catchment

Bruntland Burn is a 3.2 km$^2$ headwater catchment in the Scottish Highlands (Fig. S1). Elevation ranges between 220 and 560 m above sea level, with a wide valley bottom and steep slopes, typical of post-glacial landscapes. The bedrock (mainly granite and meta-sediments) underlies glacial drift deposits that cover 60-70% of the catchment and maintain a perennial source of base flow to the stream (Soulsby, Bradford, et al., 2016). These deposits are overlain by ~1m deep histosols (peats and peaty gleys) in the riparian area (~21% of the catchment area). The remainder (~79%) of the catchment pedology is dominated by freely-draining podzols (<0.7 m deep) on the hillslopes, while thin regosols (rankers) are found where drift deposits are marginal (above 400 masl). Spatial patterns of land cover reflect these hydropedological units. Heather shrublands (*Calluna vulgaris* and *Erica* spp.) and Scots pine (*Pinus sylvestris L.*) are the dominant vegetation over the hillslopes. The former is secondary vegetation following deforestation and subsequent overgrazing by red deer (*Cervus elaphus*) and sheep, while Scots pine forest would be the natural vegetation cover, now restricted to steeper inaccessible hillslopes and fenced plantations. Finally, grasses (*Molinia caerulea*) cover the riparian gley soils, while the peat is dominated by bog mosses (*Sphagnum* spp.). The water balance is energy-limited; annual precipitation is ~1000 mm with a slight winter maximum, about 400 mm becomes evapotranspiration (ET) with pronounced seasonality (Birkel et al., 2011). Mean annual temperature is 7 $^{o}$C and monthly-averaged temperatures remain above 0 ˚C, the climate is temperate to boreal oceanic; <5% of precipitation usually occurs as snowfall.

### 2.2 Critical Zone ecohydrological model

We used Ec$H_2$O-iso, a process-based, fully-distributed ecohydrological model designed to jointly simulate energy, water and vegetation dynamics in the critical zone (Kuppel et al., 2018a). Ec$H_2$O-iso tightly couples a two-layer energy balance scheme based on flux-gradient similarity (allowing to separately compute transpiration, evaporation of intercepted water, and soil evaporation), a hydrological module for vertical and lateral transfers (based on a 1D kinematic wave approximation for stream and groundwater), and a biomass component to simulate vegetation phenology and growth (Maneta & Silverman, 2013). Root water uptake profile is based on a parameterized exponential form across the three layers of the hydrological domain (encompassing the vadose zone and groundwater), and soil evaporation is restricted to the top layer. Ec$H_2$O-iso tracks stable isotopes ($^{2}$H and $^{18}$O) ratios in water, and water ages. For each pixel and critical zone compartment, a full-mixing mass balance equation is applied to tracers (isotopic ratios and age) at each sub-timestep when water is exchanged (and includes evaporative fractionation of isotopes; Kuppel et al., 2018a), providing a time-varying mean value. Because outgoing fluxes have the same fully-mixed tracer signature as their feeding pool(s), the mean water ages (MWA) in the former locally equates the water ages in the latter. More details on Ec$H_2$O-iso, and recent developments, can be found in Smith et al. (2019). The model was run at daily time steps using a 100x100 $m^2$ grid, from February 2013 to February 2016 (see section 2.3 and Supplementary Information).

### 2.3 Data sets and model calibration

The model has been extensively calibrated using a wide range of datasets (Kuppel et al., 2018b, 2018a). Calibration data includes stream discharge at the outlet, soil water content (5 sites, multiple depths), sapflow-derived pine stand transpiration (2 sites), top-of-canopy net radiation (3 sites), and isotope ratios ($\delta^2$H and $\delta^{18}$O) at the stream outlet, in bulk soil water (4 sites), and groundwater (4 wells), as summarised in Table S1 and detailed in Kuppel et al. (2018b, 2018a). This provided an ensemble of 30 "best runs" which satisfactorily captured catchment behavior in terms of water fluxes, stores, and velocity, as summarized in Fig. S2. A 12-yr spinup period was used during calibration to limit transient effects in the different stores, fluxes and isotopic composition. These ensemble simulations were then re-run with a 30-yr spinup, given the longer period necessary for water ages to stabilize (Fig. S3).

### 2.4 Analysis

We exclude canopy-intercepted water from our analysis of water fluxes, stores, and age dynamics. $EcH_2O$-iso does not simulate stemflow, so intercepted water does not mix with the below-canopy compartments; there is field-based evidence that it is a reasonable simplification as stemflow accounts for <1% of net precipitation here (Soulsby et al., 2017). We acknowledge that evaporation of intercepted water makes up a substantial part of evapotranspiration (ET), associated to very young ages (~38±13% of annual ET and aged a few days, not shown). In the remainder of this study, precipitation inputs are adjusted for interception losses (effective precipitation, Fig. 1a). Finally, our analysis utilizes the normalization proposed by (Zuecco et al., 2016), using the maximum and minimum values for each model realization:

$$x^{*}(t) = \frac{x(t) - min(x)}{max(x) - min(x)} \tag{1}$$

where $x$ is either water age or storage. This allows focusing on the intra-simulation seasonal dynamics for each of the catchment parameterizations in the ensemble approach adopted here, removing inter-model dispersion arising from different initial conditions after spinup.

# 3 Results

## 3.1 Catchment storage and water ages

The below-canopy catchment budget is dominated by stream discharge (Fig. 1b), yet the relative contribution of soil evaporation and transpiration is dominant during the growing season (Fig. 1c). A large predictive uncertainty surrounds the age of groundwater outputs (Fig. 1d), however this flux remains small in all ensemble simulations. As a result, we do not analyze the patterns of lateral groundwater outflow, and limit our focus to the dynamics of soil evaporation, plant transpiration, and stream outflow.

The mean water ages in streamwater and transpiration clearly exhibits an inverse storage relationship – i.e. water age since precipitation input decreases as catchment storage (including the unsaturated and saturated profile) increases, *sensu* (Harman, 2015) – across the simulation ensemble (Fig. 2a,c). However, this inverse relationship is only found during the growing season for soil evaporation, while water age time tends to increase in winter time when this flux is small (Fig. 2b). Some anticlockwise hysteresis is also clearly visible for transpiration, and to a lesser extent soil evaporation (Fig. 2a-b), meaning that for a similar storage value, these outgoing fluxes tap older water during the drying period (February to July) than during the rewetting period (August to January).

## 3.2 Preference of age extraction

We also computed the ratio between the age of water losses and the age of the water being currently stored in the catchment. This exit age ratio, hereafter EAR, is indicative of the "preference" towards younger waters (Soulsby, Birkel, et al., 2016). In other words, EAR is the degree to which each output mobilizes the youngest stores or rapid catchment flow pathways (EAR tending to 0, hereby highlighting heterogeneities) to tapping across well-mixed, less variable stores (EAR tending to 1). We find that EAR values between 0.25 and 0.5 for both green water outputs (Fig. 3a-b). We interpret the limited seasonal variations as a high synchronicity between catchment water demographics and that of extracted water, consistent with the full mixing assumptions used at grid cell level and the generally weak seasonality of catchment inputs and limited water stress in the catchment at any point of the year. By contrast, streamflow shows a preference for comparatively older water pools in the catchment, while a clear progression towards younger water extraction with increased wetness states (and high flow), then mobilizing waters half the age (or less) than those stored in the catchment.

### 3.3 Dynamics in dominant hydropedological units

The above description provides an integrated perspective at the catchment scale of the age demographics of water losses in the critical zone. However, we also seek to disentangle the interplay between local dynamics and the relative contributions in different hydropedological units. In general, a weaker control of storage on water ages is found in the valley bottom than on the hillslopes (Fig. 4a-d). In addition, the patterns for transpiration ages at the catchment scale (Fig. 2a) mostly reflect those found on the hillslopes with an inverse storage effect and hysteresis (Fig. 4a), related to the dominant contribution of Scots pine and heather shrubs transpiration covering ~80% of the catchment (in terms of spatially-aggregated budget, Fig. 4e). In the case of soil evaporation (Fig. 4c-d), these individual units displays less symmetrically V-shaped MWA* dynamics than found at the catchment scale (Fig. 2a), with a more limited increase of winter ages on the hillslopes and noisier variations on the valley bottom. We note that these normalized seasonal dynamics are relative to a baseline of younger water evapotranspired in the hillslopes than in the valley bottom (< 1 year and 1-2.5 years, respectively, Fig. S4).

## 4 Discussion

The time-variant nature of water ages from precipitation to output has been widely observed in various critical zone settings (Benettin et al., 2017; Destouni, 1991; Heidbüchel et al., 2012; Hrachowitz et al., 2015; van der Velde et al., 2012). Taking the example of a well-studied catchment, we show that while mean water ages are generally controlled by storage, seasonal patterns are significantly different between the output fluxes and the spatial scales we considered (catchment and hydropedological subunits). In particular, our approach reveals that the "inverse storage effect" defined by Harman (2015) applies to stream water ages at the catchment scale but is not a ubiquitous feature across outputs and in subcatchment units.

Water ages in catchment-scale transpiration had a rapid and inverse response to storage variations particularly visible during the driest months, at the peak of the growing season. However, the bulk of seasonal dynamics exhibited a hysteretic storage-age behavior in which spring transpiration used older water than in fall (by ~25% of the seasonal age range), despite similar catchment storage status (Fig. 2a). This seems to point to a seasonal carry-over of winter rewetting events that partially subsidize spring transpiration, while plant water use in fall relies on more recently infiltrated precipitation after summer drying. Such an asymmetrical buffering effect was less identifiable for soil evaporation where it might be obscured by short-term variability (Fig. 2b), probably owing to the fact that topsoil dynamics are more responsive to hydroclimate variability, and thus less prone to "memory effects", than the deeper layers accessible to the root water uptake. In addition, the distinctively V-shaped seasonal storage-age relationship of soil evaporation indicates the fundamentally different dynamics between the two components of evaporative losses, even at the aggregated scale first considered here, thereby pointing at the limits of only considering a single evapotranspiration term to conceptualise ecohydrological couplings driving partitioning and water budget in catchments (Fatichi et al., 2012, 2014; Vivoni, 2012). Finally, only mean water ages in streamflow displayed a consistent inverse storage effect (Fig. 2c), a feature observed in various settings (e.g. Harman, 2015; Pangle et al., 2017; Rodriguez et al., 2018), including the one studied here with independent approaches (Benettin et al., 2017). The synchronous decrease in the ratio of stream water ages to catchment-stored water ages (Fig. 3c) reflects an increasing relative contribution of recent, less-well-mixed water to the stream in wetter conditions (Harman, 2019). In other words, during the rewetting period (August to January), stream-feeding pathways increasingly bypass and outpace contribution of older, mixed water in deeper catchment stores. The associated seasonal decrease of transit times (since lateral and precipitation inputs) in the valley bottom, but also on the hillslopes in the wettest months (Fig. S5c) is consistent with the reported increase in extent of surface connectivity via saturation overland flow, first in the saturated riparian histosols and eventually including the hillslope podzols (Tetzlaff et al., 2014).

In the valley bottom, the weak seasonal variability of water ages (and in particular the lack of water ages increase in summer, Fig. 4) and markedly older baseline ages than the hillslopes (Fig. S4) translated the generally wet conditions in the riparian area, maintaining leveled soil evaporation rate throughout the months when storage is lowest (Fig. 4f and S4e). This is a result of slow-draining water subsidy from the hillslope with downslope transit time of about 6 months and even slower turnover within the valley bottom with 1-to-2 years transit times (Fig. S5a-b). The stronger (and generally inverse) constraint of storage on MWA on the hillslope reflected the higher turnover in these shallower freely-draining podzols, where the limited hydroclimatic seasonality makes green water demographics more controlled by the atmospheric demand.

These differences between subcatchment units draw attention to the interplay between local dynamics of water ages and spatial organization of contributing fluxes, whereby a range of catchment age dynamics that could be interpreted as complex mixing patterns may also be produced by time-changing lateral heterogeneity. Using the daily fraction of catchment transpiration and soil evaporation budgets taking place on the hillslope as indices of such an heterogeneity, we found that landscape organization explains around half of the catchment-scale, seasonal variability of the ages of these two green water outputs (43±25% and 53±20% across ensemble simulations, respectively, not shown). Although our numerical model uses full local mixing in each simulated compartment for each pixel, our spatially-aggregated analyses of storage and water ages essentially describe a partially-mixed system with changing macro-scale water pathways over time. Our approach thus provides an alternative to catchment-lumped analytical formulations of time-variant transit time distributions (TTD) and StorAge selection (SAS) functions and to numerical experiments testing the impact of partially-mixing flows on water ages (e.g., Cain et al., 2019; Knighton et al., 2017). All provide different perspectives on how to model the unavoidable structural and functional heterogeneity of real-world catchments (Sprenger et al., 2019), but spatially-lumped descriptions cannot fully reject the full mixing hypothesis if a complex age response can also be reproduced with spatial heterogeneity, as is the case here.

There is thus a need to assess the relative importance of preferential flows at the pore scale (Beven & Germann, 2013) and areal scales (i.e. spatial organization; Hendrickx & Flury, 2001) in the resulting catchment functioning. Our approach was limited to considering uniform flows in three hydrological layers of each grid cell, and our soil evaporation ages from a well-mixed topsoil likely underestimated the contribution of recent surface waters to this flux. Yet, combining these simplified formulations with spatially-distributed flow paths has allowed capturing water flux and tracer concentrations measured at multiple locations in several critical zone compartments of high-latitude catchments (Kuppel et al., 2018a; Smith et al., 2019). In addition, accounting for local preferential flow may not always improve catchment-scale simulations (Glaser et al., 2019; Hopp et al., 2020). The present simulations further suggest that plants access relatively old water pools (from ~6 months on the hillslopes, to over 2 years in the valley bottom, Fig. S4) with an hysteretic relationship to storage not found in streamflow ages. This modelling approach is therefore relevant to interpreting water pathways from measured tracer concentrations (Penna et al., 2018). It can help evaluating whether the proposed ecohydrological separation (Brooks et al., 2010) between tightly-bound and mobile water effectively reflects "preferential pore space selection" in root water uptake, or can be fully explained via the conservation of water masses in heterogeneously-conducting media (Berghuijs & Allen, 2019) including tree-water storage (Knighton et al., 2020; Meinzer et al., 2006).

The generic nature of hillslope-riparian couplings in real-world catchments makes our spatialized analysis of water ages relevant to identifying key contributing areas in the face of environmental changes. We show for example that hillslope transit times account for a third to half of streamflow ages at the outlet, suggesting high sensitivity of river flow to water partitioning on hillslopes. Yet, the vast majority of catchment management solutions focus on riparian management (e.g. forest felling restrictions zones around streams, or water quality buffer strips in agricultural land) as common-sense or cost-effective approaches, without often knowing the specific nature of hillslope-riparian interactions. These issues may be particularly crucial in high-latitude landscapes such as the one where this study was conducted. There, climate and land cover changes induce rapid shifts in snowfall/rainfall partition and biomes shifts. The presented ecohydrological modelling approach may help inferring the likely ecohydrological consequences of these changes, more critically so considering the general decline of high-latitude catchment monitoring (Laudon et al., 2017).

## Acknowledgments, model code, and data

The source code of the EcH$_2$O-iso model is publicly available on https://bitbucket.org/sylka/ech2o_iso/ (branch master_2.0). Input, forcing and output files, along with scripts to launch ensemble simulations and create basic plots are on a Zenodo repository (doi: 10.5281/zenodo.3592491. This work was supported by the European Research Council (ERC, project GA 335910 VeWa). M.P. Maneta acknowledges support from the NASA Ecological Forecasting Program award #80NSSC19K00181 and NASA EPSCoR #80NSSC18M0025M.

## References

Allen, S. T., Kirchner, J. W., Braun, S., Siegwolf, R. T., & Goldsmith, G. R. (2019). Seasonal origins of soil water used by trees. *Hydrology and Earth System Sciences*, *23*(2), 1199–1210.

Bales, R. C., Goulden, M. L., Hunsaker, C. T., Conklin, M. H., Hartsough, P. C., O'Geen, A. T., et al. (2018). Mechanisms controlling the impact of multi-year drought on mountain hydrology. *Scientific Reports*, *8*(1), 1–8. https://doi.org/10.1038/s41598-017-19007-0

Benettin, P., Van Der Velde, Y., Van Der Zee, S. E., Rinaldo, A., & Botter, G. (2013). Chloride circulation in a lowland catchment and the formulation of transport by travel time distributions. *Water Resources Research*, *49*(8), 4619–4632.

Benettin, P., Soulsby, C., Birkel, C., Tetzlaff, D., Botter, G., & Rinaldo, A. (2017). Using SAS functions and high-resolution isotope data to unravel travel time distributions in headwater catchments. *Water Resources Research*, *53*(3), 1864–1878.

Berghuijs, W. R., & Allen, S. T. (2019). Waters flowing out of systems are younger than the waters stored in those same systems. *Hydrological Processes*, *0*(0).

https://doi.org/10.1002/hyp.13569

Bethke, C. M., & Johnson, T. M. (2008). Groundwater Age and Groundwater Age Dating. *Annual Review of Earth and Planetary Sciences*, *36*(1), 121–152. https://doi.org/10.1146/annurev.earth.36.031207.124210

Beven, K., & Germann, P. (2013). Macropores and water flow in soils revisited. *Water Resources Research*, *49*(6), 3071–3092. https://doi.org/10.1002/wrcr.20156

Birkel, C., Tetzlaff, D., Dunn, S. M., & Soulsby, C. (2011). Using time domain and geographic source tracers to conceptualize streamflow generation processes in lumped rainfall-runoff models. *Water Resources Research*, *47*(2), W02515. https://doi.org/10.1029/2010WR009547

Bolin, B., & Rodhe, H. (1973). A note on the concepts of age distribution and transit time in natural reservoirs. *Tellus*, *25*(1), 58–62. https://doi.org/10.1111/j.2153-3490.1973.tb01594.x

Botter, G. (2012). Catchment mixing processes and travel time distributions. *Water Resources Research*, *48*(5). https://doi.org/10.1029/2011WR011160

Brooks, J. R., Barnard, H. R., Coulombe, R., & McDonnell, J. J. (2010). Ecohydrologic separation of water between trees and streams in a Mediterranean climate. *Nature Geoscience*, *3*(2), 100–104.

Cain, M. R., Ward, A. S., & Hrachowitz, M. (2019). Ecohydrologic separation alters interpreted hydrologic stores and fluxes in a headwater mountain catchment. *Hydrological Processes*, *33*(20), 2658–2675. https://doi.org/10.1002/hyp.13518

Chitra-Tarak, R., Ruiz, L., Dattaraja, H. S., Kumar, M. M., Riotte, J., Suresh, H. S., et al. (2018). The roots of the drought: Hydrology and water uptake strategies mediate forest-wide demographic response to precipitation. *Journal of Ecology*, *106*(4), 1495–1507.

Destouni, G. (1991). Applicability of the Steady State Flow Assumption for Solute Advection in Field Soils. *Water Resources Research*, *27*(8), 2129–2140. https://doi.org/10.1029/91WR01115

Douinot, A., Tetzlaff, D., Maneta, M., Kuppel, S., Schulte-Bisping, H., & Soulsby, C. (2019). Ecohydrological modelling with EcH2O-iso to quantify forest and grassland effects on water partitioning and flux ages. *Hydrological Processes*, *33*(16), 2174–2191. https://doi.org/10.1002/hyp.13480.

Evaristo, J., Kim, M., Haren, J. van, Pangle, L. A., Harman, C. J., Troch, P. A., & McDonnell, J. J. (2019). Characterizing the fluxes and age distribution of soil water, plant water, and deep percolation in a model tropical ecosystem. *Water Resources Research*. https://doi.org/10.1029/2018WR023265

Falkenmark, M., & Rockström, J. (2006). The New Blue and Green Water Paradigm: Breaking New Ground for Water Resources Planning and Management. *Journal of Water Resources Planning and Management*, *132*(3), 129–132. https://doi.org/10.1061/(ASCE)0733-9496(2006)132:3(129)

Fan, Y., Miguez-Macho, G., Jobbágy, E. G., Jackson, R. B., & Otero-Casal, C. (2017). Hydrologic regulation of plant rooting depth. *Proceedings of the National Academy of Sciences*, *114*(40), 10572–10577. https://doi.org/10.1073/pnas.1712381114

Fan, Y., Clark, M., Lawrence, D. M., Swenson, S., Band, L. E., Brantley, S. L., et al. (2019). Hillslope hydrology in global change research and Earth system modeling. *Water Resources Research*, *55*(2), 1737–1772.

Fatichi, S., Ivanov, V. Y., & Caporali, E. (2012). A mechanistic ecohydrological model to investigate complex interactions in cold and warm water-controlled environments: 2. Spatiotemporal analyses. *Journal of Advances in Modeling Earth Systems*, *4*(2). https://doi.org/10.1029/2011MS000087

Fatichi, S., Zeeman, M. J., Fuhrer, J., & Burlando, P. (2014). Ecohydrological effects of management on subalpine grasslands: From local to catchment scale. *Water Resources Research*, *50*(1), 148–164. https://doi.org/10.1002/2013WR014535

Gerke, H. H., & Van Genuchten, M. T. (1993). A dual-porosity model for simulating the preferential movement of water and solutes in structured porous media. *Water Resources Research*, *29*(2), 305–319.

Glaser, B., Jackisch, C., Hopp, L., & Klaus, J. (2019). How Meaningful are Plot-Scale Observations and Simulations of Preferential Flow for Catchment Models? *Vadose Zone Journal*, *18*(1), 180146. https://doi.org/10.2136/vzj2018.08.0146

Hahm, W. J., Dralle, D. N., Rempe, D. M., Bryk, A. B., Thompson, S. E., Dawson, T. E., & Dietrich, W. E. (2019). Low subsurface water storage capacity relative to annual rainfall decouples Mediterranean plant productivity and water use from rainfall variability. *Geophysical Research Letters*, *46*(12), 6544–6553.

Harman, C. J. (2015). Time-variable transit time distributions and transport: Theory and application to storage-dependent transport of chloride in a watershed. *Water Resources Research*, *51*(1), 1–30. https://doi.org/10.1002/2014WR015707

Harman, C. J. (2019). Age-Ranked Storage-Discharge Relations: A Unified Description of Spatially Lumped Flow and Water Age in Hydrologic Systems. *Water Resources Research*, *55*(8), 7143–7165.

Heidbüchel, I., Troch, P. A., Lyon, S. W., & Weiler, M. (2012). The master transit time distribution of variable flow systems. *Water Resources Research*, *48*(6).

Hendrickx, J. M., & Flury, M. (2001). Uniform and preferential flow mechanisms in the vadose zone. *Conceptual Models of Flow and Transport in the Fractured Vadose Zone*, 149–187.

Hopp, L., Glaser, B., Klaus, J., & Schramm, T. (2020). The relevance of preferential flow in catchment scale simulations: Calibrating a 3D dual-permeability model using DREAM. *Hydrological Processes*, *34*(5), 1237–1254. https://doi.org/10.1002/hyp.13672

Hrachowitz, M., Savenije, H., Bogaard, T. A., Soulsby, C., & Tetzlaff, D. (2013). What can flux tracking teach us about water age distribution patterns and their temporal dynamics? *Hydrology and Earth System Sciences, 17 (2), 2013*.

Hrachowitz, M., Fovet, O., Ruiz, L., & Savenije, H. H. G. (2015). Transit time distributions, legacy contamination and variability in biogeochemical 1/fα scaling: how are hydrological response dynamics linked to water quality at the catchment scale? *Hydrological Processes*, *29*(25), 5241–5256. https://doi.org/10.1002/hyp.10546

Hrachowitz, M., Benettin, P., Van Breukelen, B. M., Fovet, O., Howden, N. J., Ruiz, L., et al. (2016). Transit times—The link between hydrology and water quality at the catchment scale. *Wiley Interdisciplinary Reviews: Water*, *3*(5), 629–657.

Jasechko, S. (2019). Global Isotope Hydrogeology―Review. *Reviews of Geophysics*, *57*(3), 835–965. https://doi.org/10.1029/2018RG000627

Jasechko, S., Kirchner, J. W., Welker, J. M., & McDonnell, J. J. (2016). Substantial proportion of global streamflow less than three months old. *Nature Geoscience*, *9*(2), 126–129. https://doi.org/10.1038/ngeo2636

Kirchner, J. W. (2016). Aggregation in environmental systems–Part 1: Seasonal tracer cycles quantify young water fractions, but not mean transit times, in spatially heterogeneous catchments. *Hydrology and Earth System Sciences*, *20*(1), 279–297.

Knighton, J., Saia, S. M., Morris, C. K., Archiblad, J. A., & Walter, M. T. (2017). Ecohydrologic considerations for modeling of stable water isotopes in a small intermittent watershed. *Hydrological Processes*, *31*(13), 2438–2452. https://doi.org/10.1002/hyp.11194

Knighton, J., Kuppel, S., Smith, A., Soulsby, C., Sprenger, M., & Tetzlaff, D. (2020). Using isotopes to incorporate tree water storage and mixing dynamics into a distributed ecohydrologic modelling framework. *Ecohydrology*, *n/a*(n/a), e2201. https://doi.org/10.1002/eco.2201

Kuppel, S., Fan, Y., & Jobbágy, E. G. (2017). Seasonal hydrologic buffer on continents: Patterns, drivers and ecological benefits. *Advances in Water Resources*, *102*, 178–187. https://doi.org/10.1016/j.advwatres.2017.01.004

Kuppel, S., Tetzlaff, D., Maneta, M. P., & Soulsby, C. (2018a). EcH2O-iso 1.0: water isotopes and age tracking in a process-based, distributed ecohydrological model. *Geoscientific Model Development*, *11*(7), 3045–3069. https://doi.org/10.5194/gmd-11-3045-2018

Kuppel, S., Tetzlaff, D., Maneta, M. P., & Soulsby, C. (2018b). What can we learn from multi-data calibration of a process-based ecohydrological model? *Environmental Modelling & Software*, *101*, 301–316. https://doi.org/10.1016/j.envsoft.2018.01.001

Maneta, M. P., & Silverman, N. L. (2013). A spatially distributed model to simulate water, energy, and vegetation dynamics using information from regional climate models. *Earth Interactions*, *17*(11), 1–44.

Maneta, M. P., Soulsby, C., Kuppel, S., & Tetzlaff, D. (2018). Conceptualizing catchment storage dynamics and nonlinearities. *Hydrological Processes*, *32*(21), 3299–3303.

McGuire, K. J., & McDonnell, J. J. (2015). Tracer advances in catchment hydrology. *Hydrological Processes*, *29*(25), 5135–5138. https://doi.org/10.1002/hyp.10740

Meinzer, F. C., Brooks, J. R., Domec, J.-C., Gartner, B. L., Warren, J. M., Woodruff, D. R., et al. (2006). Dynamics of water transport and storage in conifers studied with deuterium and heat tracing techniques. *Plant, Cell & Environment*, *29*(1), 105–114.

Penna, D., Hopp, L., Scandellari, F., Allen, S. T., Benettin, P., Beyer, M., et al. (2018). Ideas and perspectives: Tracing terrestrial ecosystem water fluxes using hydrogen and oxygen stable isotopes – challenges and opportunities from an interdisciplinary perspective. *Biogeosciences*, *15*(21), 6399–6415. https://doi.org/10.5194/bg-15-6399-2018

Remondi, F., Kirchner, J. W., Burlando, P., & Fatichi, S. (2018). Water Flux Tracking With a Distributed Hydrological Model to Quantify Controls on the Spatio-temporal Variability of Transit Time Distributions. *Water Resources Research*, *54*(4), 3081–3099. https://doi.org/10.1002/2017WR021689

Rinaldo, A., Benettin, P., Harman, C. J., Hrachowitz, M., McGuire, K. J., Van Der Velde, Y., et al. (2015). Storage selection functions: A coherent framework for quantifying how catchments store and release water and solutes. *Water Resources Research*, *51*(6), 4840–4847.

Smith, A., Tetzlaff, D., Laudon, H., Maneta, M., & Soulsby, C. (2019). Assessing the influence of soil freeze–thaw cycles on catchment water storage–flux–age interactions using a tracer-aided ecohydrological model. *Hydrology and Earth System Sciences*, *23*(8), 3319–3334. https://doi.org/10.5194/hess-23-3319-2019

Soulsby, C., Birkel, C., Geris, J., Dick, J., Tunaley, C., & Tetzlaff, D. (2015). Stream water age distributions controlled by storage dynamics and nonlinear hydrologic connectivity: Modeling with high-resolution isotope data. *Water Resources Research*, *51*(9), 7759–7776.

Soulsby, C., Birkel, C., & Tetzlaff, D. (2016). Characterizing the age distribution of catchment evaporative losses. *Hydrological Processes*, *30*(8), 1308–1312.

Soulsby, C., Bradford, J., Dick, J., McNamara, J. P., Geris, J., Lessels, J., et al. (2016). Using geophysical surveys to test tracer-based storage estimates in headwater catchments. *Hydrological Processes*, *30*(23), 4434–4445.

Soulsby, C., Braun, H., Sprenger, M., Weiler, M., & Tetzlaff, D. (2017). Influence of forest and shrub canopies on precipitation partitioning and isotopic signatures. *Hydrological Processes*, *31*(24), 4282–4296. https://doi.org/10.1002/hyp.11351

Sprenger, M., Stumpp, C., Weiler, M., Aeschbach, W., Allen, S. T., Benettin, P., et al. (2019). The Demographics of Water: A Review of Water Ages in the Critical Zone. *Reviews of Geophysics*, *57*(3), 800–834. https://doi.org/10.1029/2018RG000633

Tetzlaff, D., Birkel, C., Dick, J., Geris, J., & Soulsby, C. (2014). Storage dynamics in hydropedological units control hillslope connectivity, runoff generation, and the evolution of catchment transit time distributions. *Water Resources Research*, *50*(2), 969–985.

van der Velde, Y., Torfs, P. J. J. F., van der Zee, S. E. A. T. M., & Uijlenhoet, R. (2012). Quantifying catchment-scale mixing and its effect on time-varying travel time distributions. *Water Resources Research*, *48*(6). https://doi.org/10.1029/2011WR011310

Vivoni, E. R. (2012). Diagnosing seasonal vegetation impacts on evapotranspiration and its partitioning at the catchment scale during SMEX04–NAME. *Journal of Hydrometeorology*, *13*(5), 1631–1638.

Wilusz, D. C., Harman, C. J., Ball, W. B., Maxwell, R. M., & Buda, A. R. (2020). Using particle tracking to understand flow paths, age distributions, and the paradoxical origins of the inverse storage effect in an experimental catchment. *Water Resources Research*, *n/a*(n/a), e24397. https://doi.org/10.1029/2019WR025140

Yang, J., Heidbüchel, I., Musolff, A., Reinstorf, F., & Fleckenstein, J. H. (2018). Exploring the dynamics of transit times and subsurface mixing in a small agricultural catchment. *Water Resources Research*, *54*(3), 2317–2335.

Zuecco, G., Penna, D., Borga, M., & van Meerveld, H. J. (2016). A versatile index to characterize hysteresis between hydrological variables at the runoff event timescale. *Hydrological Processes*, *30*(9), 1449–1466.

**Figure 1.** (**a**) Daily catchment-aggregated time series of the below-canopy water budget at Bruntland Burn. Outputs are decomposed into soil evaporation, transpiration, stream and groundwater discharge –note the right y-axis for stream discharge– (**b**), showing their relative contributions to below-canopy outputs (**c**), and mean water ages (**d-e**). Errors bars (a) and ribbons (a-e) show the 80% intervals across the simulation ensemble.

**Figure 2**. (**a-c**) Spatially-aggregated plots of normalized mean water ages (MWA*) in plant transpiration(**a**), soil evaporation (**b**), and outlet stream discharge **(c)** versus normalized catchment storage ($S^*_{catchment}$). For each day of the year (color scale), multi-year means (02/2013 – 02/2016 period) are shown using cross-ensemble medians (small points) and 50% confidence ellipses. Open triangles indicate the normalized median storage value for each simulation. (**d**) Mean seasonal cycle of each flux contribution to the below-canopy outputs (80% interval across the simulation ensemble).

**Figure 3**. Spatially-aggregated plots of exit age ratio (EAR, the ratio between the age of water in outputs and that of water currently stored in the critical zone) of plant transpiration (**a**), soil evaporation (**b**), and outlet stream discharge **(c)** versus the normalized catchment storage ($S^*_{catchment}$). For each day of the year (color scale), multi-year means (02/2013 – 02/2016 period) are shown using cross-ensemble medians (small points) and 50% confidence ellipses. Open triangles indicate the normalized median storage value for each simulation.

**Figure 4.** (**a-b**) Spatially-aggregated plots of normalized mean water ages (MWA*) of transpiration against the normalized storage (S*) state of the subsurface, both spatially aggregated over two sub-catchment units: the hillslopes overlain by podzolic and ranker soils (**a**, ~80% of the area), and the valley bottom overlain by peat/peaty gley soils (**b**, ~20% of the area). (**c-d**) Same as (a-b) with the MWA* of soil evaporation. For each day of the year (color scale), multi-year means (02/2013 – 02/2016 period) are shown using cross-ensemble medians (small points) and 50% confidence ellipses. Open triangles indicate the normalized median storage value for each simulation. **(e-f)** Mean seasonal cycle of the contributions of soil evaporation (e) and plant transpiration (f) to catchment-scale below-canopy outputs (80% interval across the simulation ensemble); note the difference of vertical scale between panel (e) and (f).

**Figure 1.**

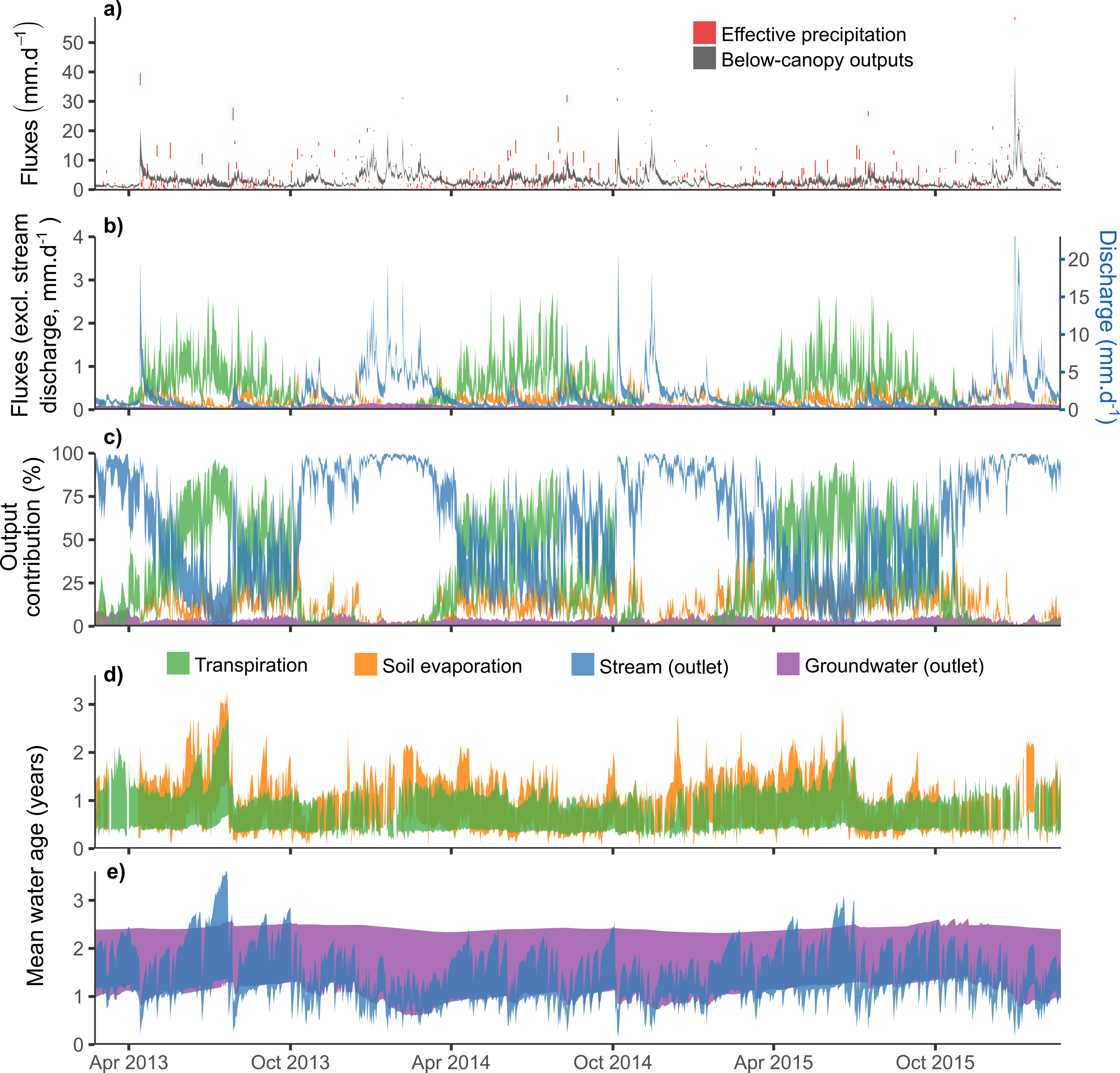

a)
Effective precipitation
Below-canopy outputs
Fluxes (mm.d$^{-1}$)
b)
Fluxes (excl. stream discharge, mm.d$^{-1}$)
Discharge (mm.d$^{-1}$)
c)
Output contribution (%)
Transpiration
Soil evaporation
Stream (outlet)
Groundwater (outlet)
d)
e)
Mean water age (years)
Apr 2013
Oct 2013
Apr 2014
Oct 2014
Apr 2015
Oct 2015

**Figure 2.**

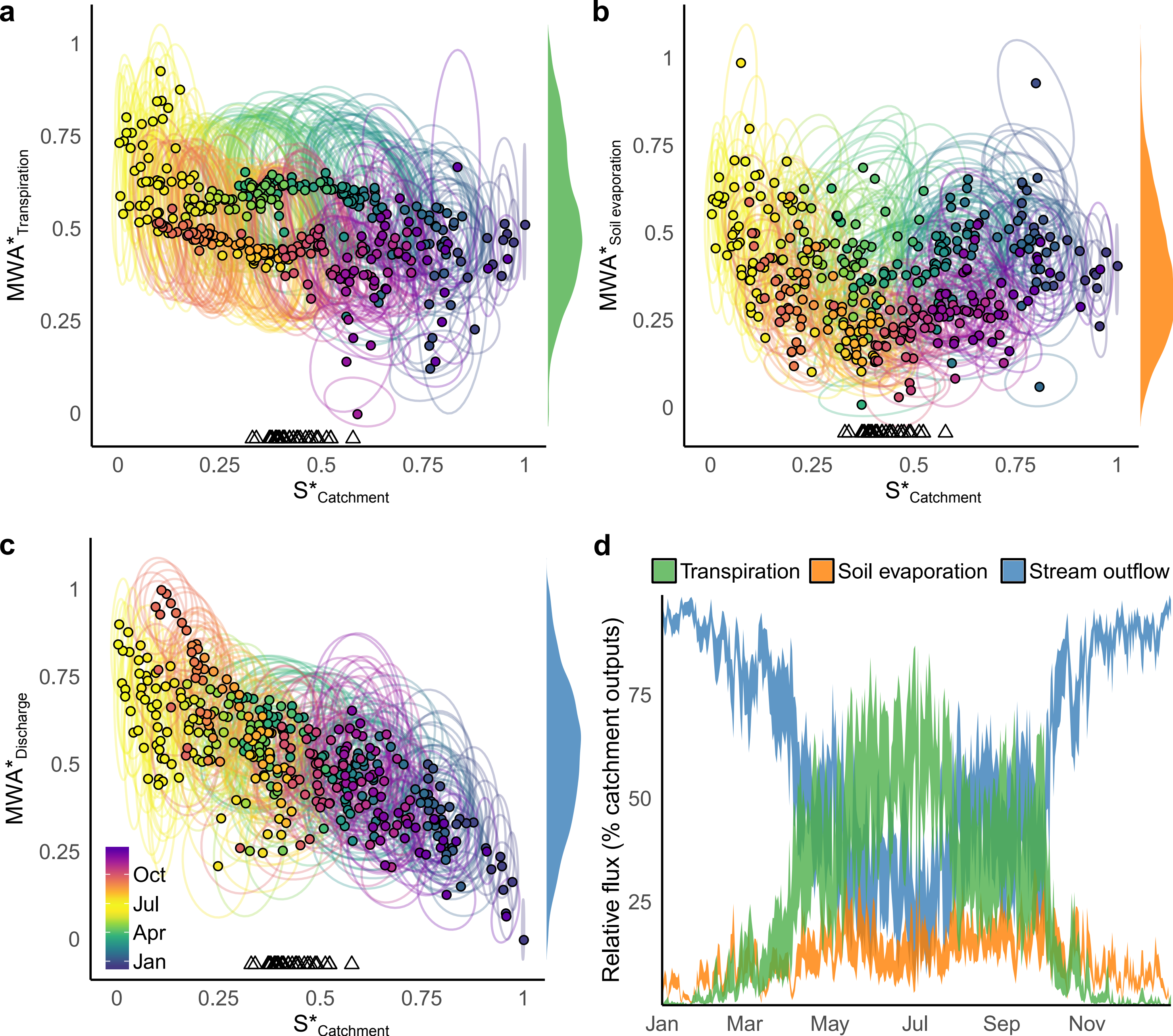

a
b
c
d
MWA*Transpiration
MWA*Soil evaporation
MWA*Discharge
S*Catchment
0
0.25
0.5
0.75
1
Oct
Jul
Apr
Jan
Transpiration
Soil evaporation
Stream outflow
Relative flux (% catchment outputs)
25
50
75
Jan
Mar
May
Jul
Sep
Nov

**Figure 3.**

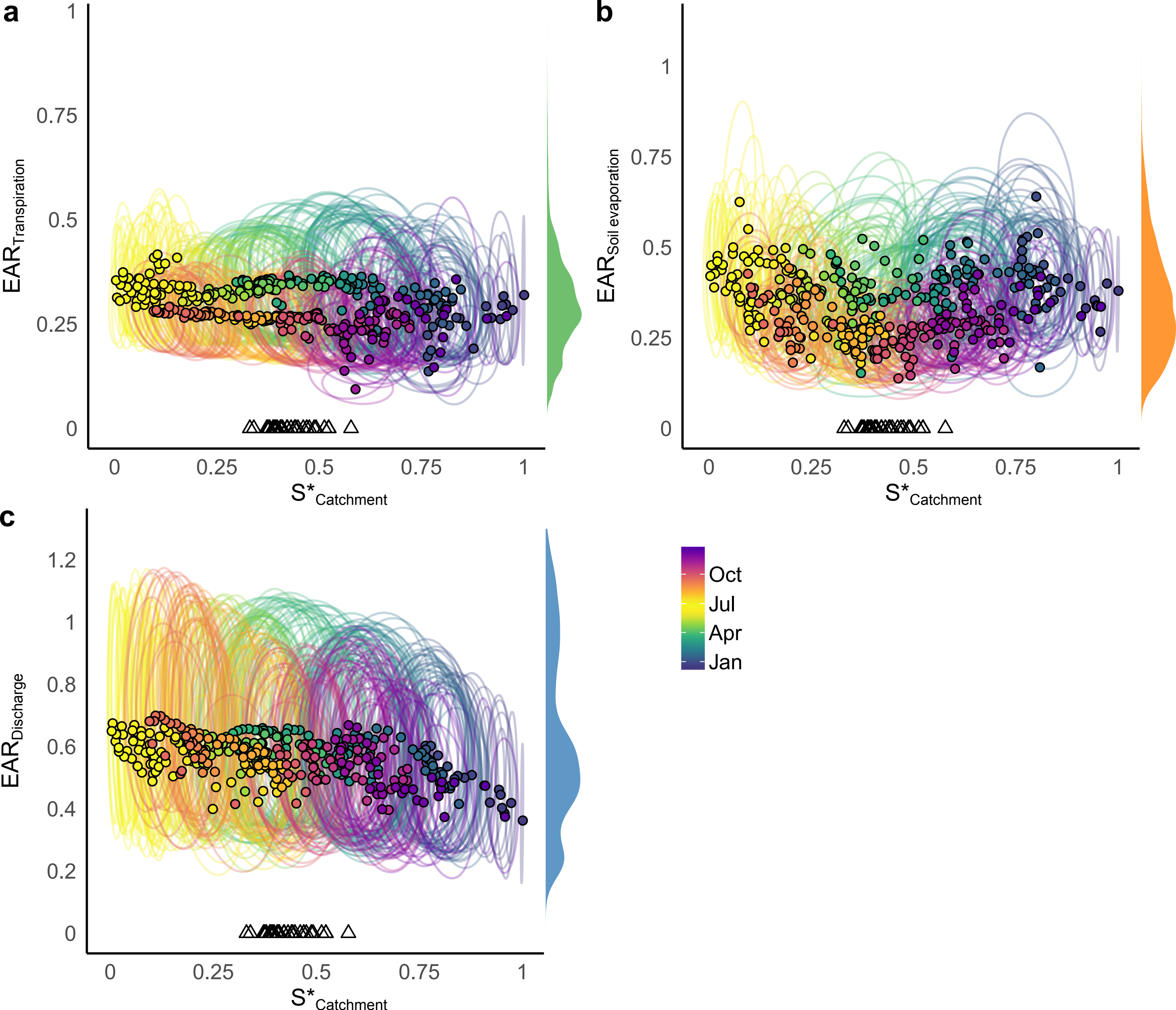

a
b
c
EAR$_{Transpiration}$
EAR$_{Soil\ evaporation}$
EAR$_{Discharge}$
S*$_{Catchment}$
0
0.25
0.5
0.75
1
1.2
0.8
0.6
0.4
0.2
Oct
Jul
Apr
Jan

**Figure 4.**

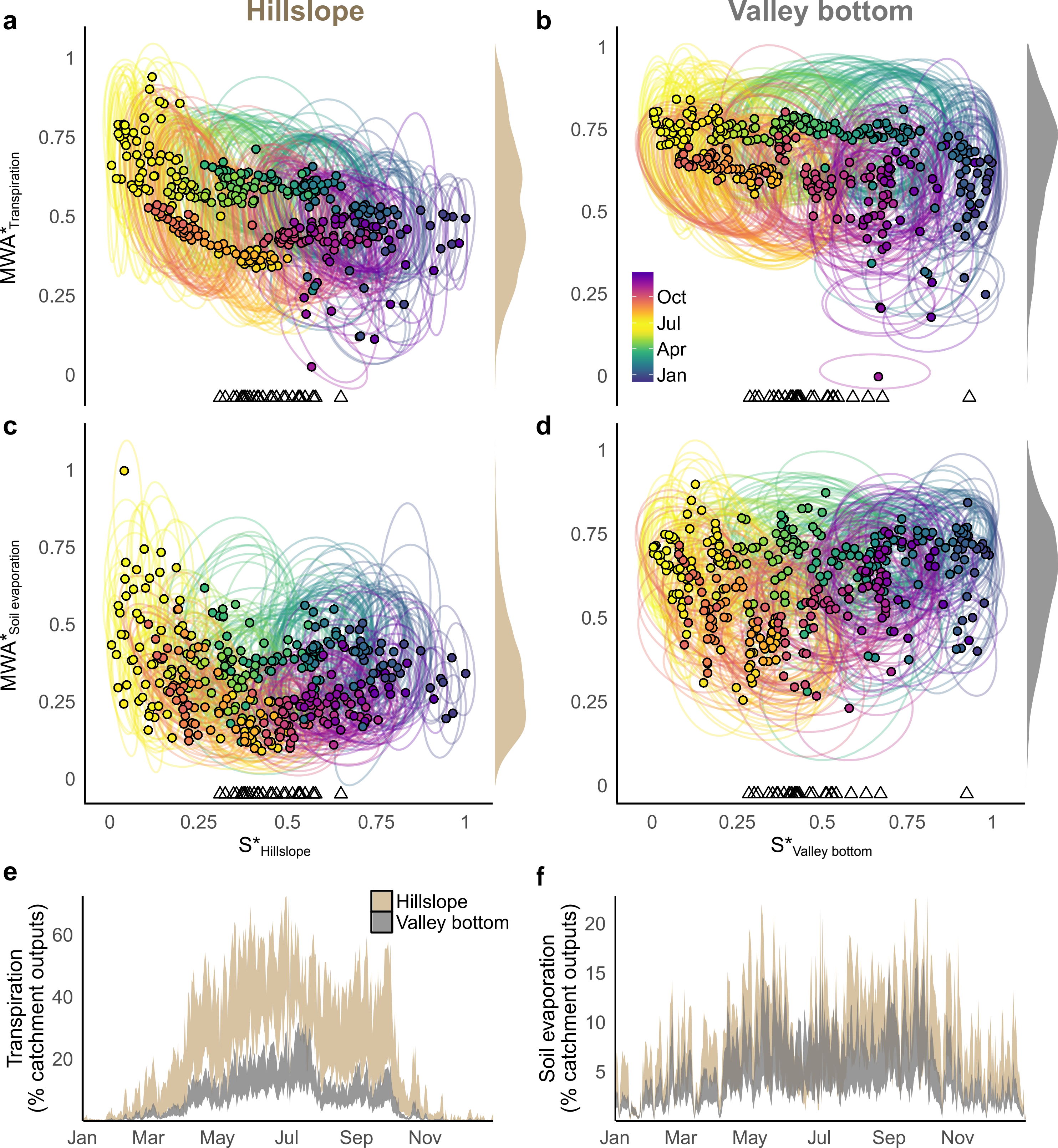
a
Hillslope
b
Valley bottom
MWA*Transpiration
1
0.75
0.5
0.25
0
Oct
Jul
Apr
Jan
c
d
MWA*Soil evaporation
S*Hillslope
S*Valley bottom
0.25
0.5
0.75
1
e
f
Hillslope
Valley bottom
Transpiration
(% catchment outputs)
60
40
20
Soil evaporation
(% catchment outputs)
20
15
10
5
Jan
Mar
May
Jul
Sep
Nov